

Learnable Fractal Flames

Jordan J. Bannister
jordan.bannister@mila.quebec
Mila - Quebec AI Institute
Montréal, QC, Canada

Derek Nowrouzezahrai
derek@cim.mcgill.ca
McGill University
Montréal, QC, Canada



Figure 1: Two fractal flames learned using our differentiable fractal rendering approach. The reference images are displayed in the top left of each frame. Left: a non-linear fractal flame based on "Fighting Forms" by Franz Marc. Right: a linear fractal flame based on "Wisteria" by Claude Monet.

ABSTRACT

This work presents a differentiable rendering approach that allows latent fractal flame parameters to be learned from image supervision. The approach extends the state-of-the-art in differentiable fractal rendering through support for color images, non-linear generator functions, and multi-fractal compositions. With these additions, differentiable rendering is now a viable tool for the generation of fractal artwork.

CCS CONCEPTS

• **Applied computing** → **Media arts**; • **Computing methodologies** → **Learning latent representations**.

KEYWORDS

Fractal Flame, Differentiable Rendering

1 INTRODUCTION

The term "fractal" was first introduced by Benoit Mandelbrot in 1975 to describe a type of geometric pattern observed in both mathematics and nature [Mandelbrot 1975]. In addition to having interesting

and useful mathematical properties, fractals have captured the attention of many artists due to their complex and beautiful aesthetic features.

Iterated function systems (IFS) are a class of methods that can be used to construct fractals. IFS fractals were first conceived in 1981 by John E. Hutchinson [Hutchinson 1981] and were brought into greater prominence by Michael Barnsley [Barnsley 2012]. As suggested by the name, a set of functions $F = \{f : X \rightarrow X\}$ define an IFS fractal. In this work, we will restrict ourselves to 2-dimensional fractals where $X = \mathbb{R}^2$. An IFS fractal can be visualized by running an algorithm called the chaos game, which proceeds as follows. First, an initial sample $s_0 \in X$ is selected. Next, for as many iterations as desired, a function $f \in F$ is used to generate another sample such that $s_i = f(s_{i-1})$. In each iteration, the function f is chosen randomly from F . Finally, the sample positions $\{s_0, s_1, s_2, \dots\}$ are plotted to create an image.

The first IFS fractals used linear generator functions and produced binary or grayscale images (see Figure 2). In 1992, Scott Draves introduced the fractal flame algorithm which greatly expanded the aesthetic range of IFS fractals [Draves and Draves 2010; Draves and Reckase 2008]. The three core ideas introduced by

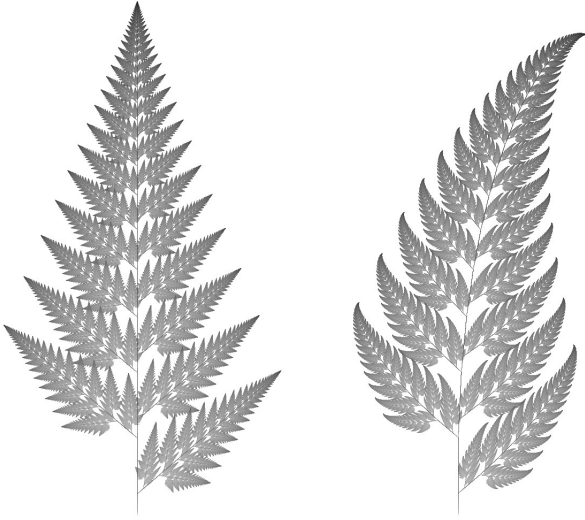


Figure 2: The Barnsley fern is an example of a linear IFS fractal. When the parameters of the generator functions are perturbed (left vs. right) the fractal structure is affected.

fractal flames are 1) the use of non-linear generator functions, 2) a log-density tone mapping approach, and 3) a method of coloring samples based on the most recent generator functions from which they were produced. Subsequently, several software programs were developed for creating and editing fractal flame art including Apophysis [Sdobnov et al. 2009], Electric Sheep [Draves 1999], JWildfire [Maschke 2001], and Chaotica [Glare Technologies 2015]. Fractal flames are now a widely known and widely used approach for creating fractal art.

In this work, we study the inverse problem of fractal flame generation. In other words, given a target image, we find the latent parameters of a fractal flame such that the generated fractal resembles the target image. We believe that this approach is valuable as an artistic tool which allows artists to use reference images to guide the generation of fractal art.

1.1 Related work

In this work, we follow the path of [Tu et al. 2023] who recently presented the first approach for learning IFS fractal parameters by gradient descent. Their core contribution was to propose a differentiable method for rendering point samples produced by the chaos game. The classic approach to rendering an IFS sample is to increment the pixel within which the sample position falls by some fixed amount. Instead, they increment pixels in a neighborhood of the sample position according to the distance from the sample to each pixel center, weighted by a radial basis function. In this approach, the fractal image pixel values are continuously related to the sample positions, thereby enabling gradient back-propagation. They liken their approach to the differentiable soft quantization module of [Qian et al. 2020] and we will note that it also bears similarity to splatting operations found in some work on differentiable triangle rasterization [Cole et al. 2021].

1.2 Contributions

The approach demonstrated by [Tu et al. 2023] has several important limitations as a tool for creating fractal art. First, the approach uses only linear generator functions. As demonstrated by the fractal flame algorithm, the use of non-linear generator functions greatly expands the aesthetic range of IFS fractals. Second, color images are not supported in their approach. Color is an essential aspect of most visual artistic creations. Finally, their approach can often struggle to accurately represent complex images.

In this work, we extend the differentiable rendering approach of [Tu et al. 2023] and address the limitations described above. Our approach can learn colorful IFS fractals with non-linear generator functions. Furthermore, we demonstrate the use of a differentiable compositor to combine multiple fractal flames for more representational flexibility. The results show that differentiable IFS fractal rendering is now a viable artistic tool.

2 OVERVIEW AND IMPLEMENTATION

A high level flow diagram of our differentiable rendering pipeline is shown in Figure 3. There are four main components. In this section, each component will be described, including inputs, outputs, parameters and other important considerations. Our implementation relies on the Taichi language [Hu et al. 2019], which supports both automatic differentiation and GPU acceleration. The code is publicly available on Github¹.

2.1 Sampler

The role of a sampler is to run the chaos game algorithm. Therefore, each sampler is associated with a set of N_F generator functions $F = \{f_i : X \rightarrow X | i = 1, \dots, N_F\}$ with trainable parameters θ_i . The number of generators and the structure of each generator function is defined when constructing the sampler. The functions in F may be non-linear, but must be differentiable.

In the original chaos game algorithm, the generator functions are randomly sampled in each iteration. In a differentiable rendering approach, we must slightly re-organize this process to ensure differentiability. Following [Tu et al. 2023], we sample the generator order separately from the generation of samples, similar to the re-parameterization trick used in variational auto-encoders [Kingma and Welling 2014]. Thus, the random sampling is treated as constant during back-propagation and the gradient flow circumvents the non-differentiable stochastic process. We perform this sampling once when first constructing the sampler, but it could also be re-performed after any parameter update. The generator order is, therefore, an array of indices $G = \{g_i \in \{1, \dots, N_F\} | i = 1, \dots, N_S\}$ where N_S is the number of samples generated. An important consequence of this re-organization is that the generator function order and the distribution from which it is sampled are not learnable.

One output of the sampler is a set of N_S sample positions $S = \{s_i \in X | i = 1, \dots, N_S\}$. The sample positions are computed by serially applying the generator functions in the order defined by the array G (Equation 1).

$$s_i = f_{g_i}(s_{i-1}) \quad (1)$$

¹anonymous link.

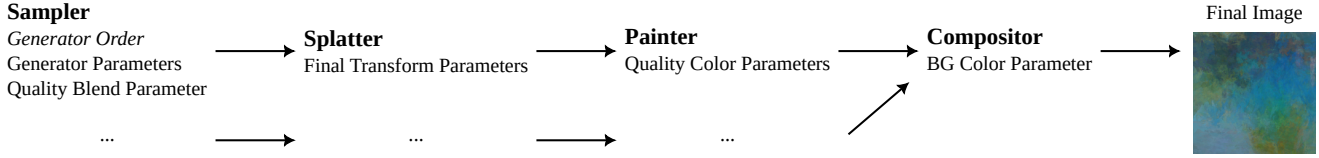


Figure 3: A flow diagram of our differentiable fractal rendering pipeline. First, a sampler produces an array of sample positions and quality vectors. Second, a splatter splats each sample quality vector onto an image buffer at the corresponding sample position. Third, a painter maps the vector at each splat buffer pixel to an RGBA value. Finally, the compositor composites one or more RGBA buffers over a background color to produce the final image. The pipeline is end-to-end differentiable.

A second output of the sampler is a set of sample quality vectors $\{q_i \in \mathbb{R}^{N_F} | i = 1, \dots, N_S\}$ in correspondence with the sample positions. The sample quality vectors (calculated using Equation 2) reflect which functions have most recently acted upon the sample.

$$q_i = \sum_{j=0}^i \kappa^{j-i} e_{g_j} \quad (2)$$

Here, e_{g_j} represents a one-hot vector with a one at the index corresponding to the generator index g_j of sample j . The learnable parameter κ represents the quality blend parameter and controls how quickly the influence of a generator function decays from the sample quality as more generator functions are applied to the sample. Parameter κ is learnable and is constrained to be greater than 1.

In our implementation, we run many versions of the serial process described above in parallel to make full use of GPU hardware. This is omitted from our notation for the sake of clarity.

2.2 Splatter

The role of a splatter is to take the outputs of a sampler, and to splat the sample quality vectors onto an image buffer at positions defined by the sample positions. The output of the splatter is, therefore, a 2D image buffer where each pixel has N_F channels. A splatter has learnable parameters that correspond to the final transform described in [Draves and Reckase 2008]. This linear transform is applied to all sample positions before they are mapped to pixel space coordinates. After a sample position has been mapped to pixel space coordinates, a center pixel (within whose bounds the sample position falls) is identified, and the sample is splatted in the 3×3 pixel neighborhood of the center pixel. Each pixel in the 3×3 neighborhood is incremented by the quality vector of the sample multiplied by a weight. The weight of a sample at a pixel whose center is d pixels distant from the sample is e^{-2d^2} . This corresponds to an isotropic Gaussian kernel with standard deviation $\sigma = 0.5$ pixels.

While there is a difference in implementation, this splatting approach uses the same general idea as [Tu et al. 2023]. The splatted pixel values are continuously related to the sample positions, thereby allowing gradient back-propagation. In our implementation, each sample is processed in parallel and accumulated into the splat buffer using atomic operations.

2.3 Painter

The role of a painter is to transform the vector q_{xy} at each pixel of the splat buffer into an RGBA pixel p_{xy} . A painter is associated with one RGBA parameter for each generator function $C = \{c_i \in \mathbb{R}^4 | 0 \leq c_i \leq 1, i = 0, \dots, N_F\}$. First, for each pixel in the splat buffer, the splat weight $w_{xy} = \text{sum}(q_{xy})$ is computed, and the maximum value w_{\max} across the splat buffer is stored. Next, for each pixel, a weight alpha $\alpha_{xy} = \log(w_{xy}) \div \log(w_{\max})$ is computed. Finally, the RGBA value p_{xy} of each pixel is computed using Equation 3.

$$p_{xy} = \frac{\alpha_{xy}}{w_{xy}} \sum_{i=0}^{N_F} c_i \cdot q_{xy_i} \quad (3)$$

It is notable that there are two sources of transparency in this approach. The first is the learnable alpha values of parameters in C . The second is the splat weight alpha α_{xy} . We also note that this approach, based on the log-density approach described in [Draves and Reckase 2008], is an ad-hoc tone mapping method with learnable parameters. Any differentiable function of the form $\mathbb{R}^{N_F} \rightarrow \mathbb{R}^4$, which outputs an RGBA value could be applied here.

2.4 Compositor

The final module in our differentiable fractal rendering pipeline is a differentiable compositor. A compositor is associated with a learnable RGB background color parameter. The role of the compositor is to composite one or more RGBA buffers over the background color. There is only one compositor in any pipeline, while there may be one or more of the other components (see Figure 3).

2.5 Training and Evaluation

Different considerations apply when optimizing fractal parameters compared to generating a final image. When training, speed of execution is critical. When generating a final image, the quality of the output is most important, and it is acceptable to increase runtime. Therefore, we set hyper-parameters to control the quality-speed trade-off separately for each scenario. When training, we use fewer samples and lower image resolution. After learning the fractal parameters, we generate a full resolution image using many more samples to ensure a high quality result.

3 EXPERIMENTS AND RESULTS

In our experiments, we aim to demonstrate that our differentiable rendering approach is a viable and useful tool for fractal art creation. All experiments were performed on an Nvidia 2070 Super GPU. The

most computationally expensive experiments, in which multi-flame fractals are trained to emulate paintings, complete in roughly 20 minutes. The simpler experiments complete in one or two minutes. For all experiments, the number of samples per flame used during training was 10^6 , and during evaluation 10^{10} . A mean squared error loss function and a vanilla gradient descent optimizer were used in all experiments.

3.1 Learning Non-Linear Flames

In Scott Draves' description of the fractal flame algorithm [Draves and Reckase 2008], 48 different non-linear generator function variations were introduced. Each of these variations can be combined with others in an infinite number of different ways. In our formulation, each generator need only be a differentiable function $f : X \rightarrow X$, which leaves substantial room for experimentation and exploration. Accepting that a comprehensive study of this space is impossible, we first demonstrate our approach using a small selection of non-linear variations.

Figure 4 shows a reference image alongside optimized fractals representing a linear variation and 6 non-linear variations. Many of these fractals are not capable of capturing the structure of the reference image closely. This is especially true when the intrinsic structure of the fractal does not match the reference image. Nevertheless, they all show a tendency to assign color and density to appropriate areas of the image. In these experiments, the background color of the image was set to white and was not learned. Each fractal was trained at a resolution of 100x100 pixels and has 8 generator functions.

3.2 Learning Multi-Flame Art

Next, we trained multi-flame fractals to emulate two famous paintings in the public domain ("Fighting Forms" by Franz Marc [Marc 1914], and "Wisteria" by Claude Monet [Monet 1925]). The results are shown in Figure 1. For Wisteria, we composed four layers of linear fractal flames with 24 generator functions each. For Fighting Forms, we composed 3 layers of non-linear fractal flames including spherical, hankerchief, and exponential variations. Both fractals were trained at a resolution of 200x200 pixels. In this experiment, we found that our pipeline was capable of capturing the gross structure of the reference image quite closely, while still exhibiting fractal aesthetic qualities.

3.3 Exploring Hyper-Parameter Effects

Next, we explored the effects associated with altering the training image resolution. The non-linear Fighting Forms fractal experiment was re-created using a training image resolution of 50x50 pixels instead of 200x200 pixels (Figure 5). The effect was to produce a fractal with significantly more thin and sharp structures compared to the original experiment. Because samples are grouped together in larger pixels at lower resolutions, the optimization process does not encourage samples to spread out to the same degree. Figure 6 replicates this effect in a linear fractal trained on the same simple reference image as in Figure 4 using a resolution of 20x20 pixels instead of 100x100 pixels.

We also explored the effects associated with altering the number of generator functions in a fractal flame. The linear Wisteria

fractal experiment was re-created using 8 generator functions for each flame instead of 24 (Figure 5). The effect was to produce a fractal with simpler structure and color palette. This effect is quite intuitive as reducing the number of generator functions reduces the number of parameters in the sampler, as well as the number of color parameters in the painter. Figure 6 replicates this effect in a linear fractal trained on the same simple reference image as in Figure 4 using 3 generator functions instead of 8. Interestingly, the simpler fractal converged to a warped version of the Sierpinski triangle.

Finally, we explored the use of different generator function variations in a multi-flame pipeline. Figure 7 shows fractal images trained on Fighting Forms and Wisteria using different non-linear variations. Each image reflects the gross structure of the reference image while retaining the fractal aesthetics of the different variations. These experiments used a composition of 3 fractal flames with 24 functions each, trained at a resolution of 200x200 pixels

4 LIMITATIONS

The differentiable fractal rendering approach described here has several limitations. First, the loss landscape associated with learning IFS fractal parameters is highly non-convex. This means that the initial configuration of parameters has a strong effect on the final result. While we were able to learn interesting and aesthetic fractals from random initialization, we occasionally needed to play with the randomization settings or random seed before we arrived at a satisfactory result. For this reason, we believe that combining a differentiable rendering approach with the manual editing of fractal parameters will likely be the approach with the most artistic utility.

Another limitation of our approach is the potential for training instability when using non-linear variations. In practice, we found that this was rarely an issue. However, we did not explore all possible variations and stability issues may still be encountered in some scenarios.

A limitation with our current fractal flame implementation is a lack of support for stochastic generator functions. In addition to using random number generation when determining the generator function order, some of the fractal flame variations also include random number generation in the generator functions themselves [Draves and Reckase 2008]. Because differentiating through stochastic sampling is not possible, supporting such flame variations would require another application of the re-parameterization trick.

5 CONCLUSION AND FUTURE WORK

In this work, we extended the state-of-the-art differentiable IFS fractal rendering approach to support non-linear generator functions, color images, and multi-flame compositions. Our experiments show that differentiable rendering is now a viable approach for creating fractal art. Overall, we believe that combining differentiable rendering with generative simulations is a fascinating area of research that can empower artists with new creative tools. Future work may explore higher dimensional IFS fractals, other fractal varieties, and other types of generative simulations. We hope that our work will inspire others to explore this space as well.

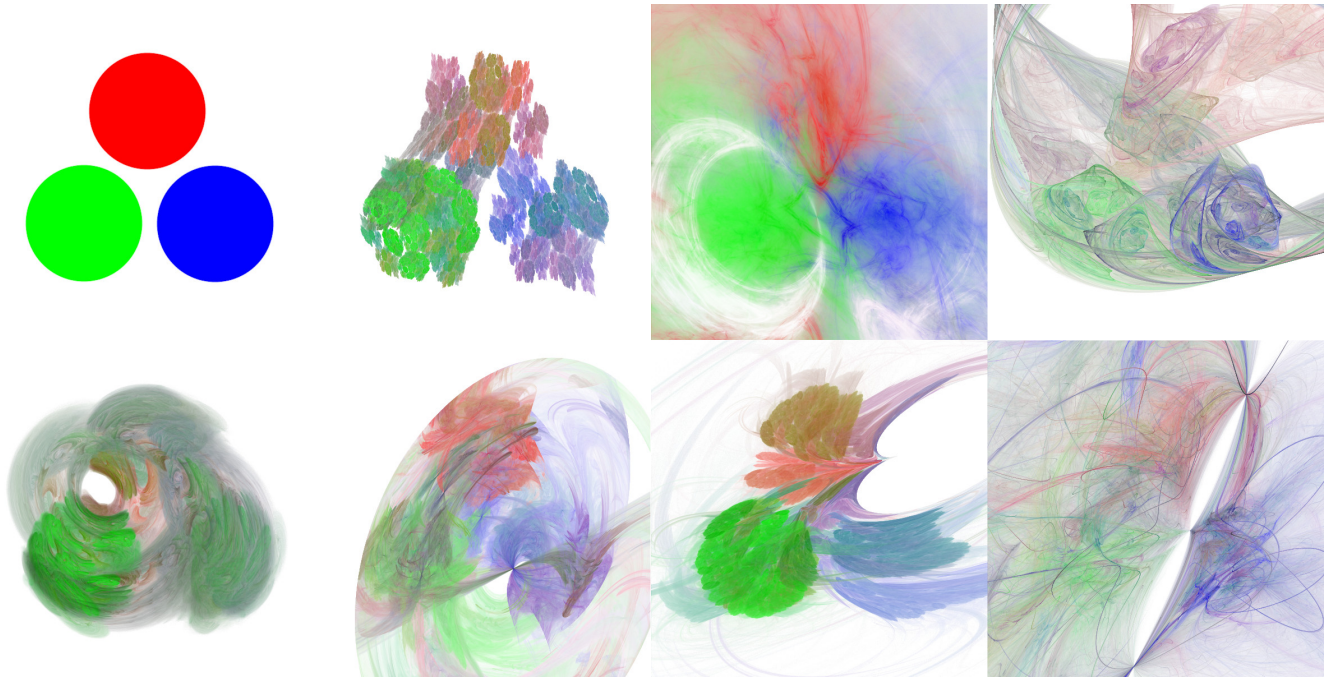


Figure 4: Fractal flames learned from a simple reference image. Top row (left to right): the reference image, a linear variation, a spherical variation, a hankerchief variation. Bottom row (left to right): an exponential variation, a disk variation, a heart variation, a power variation.

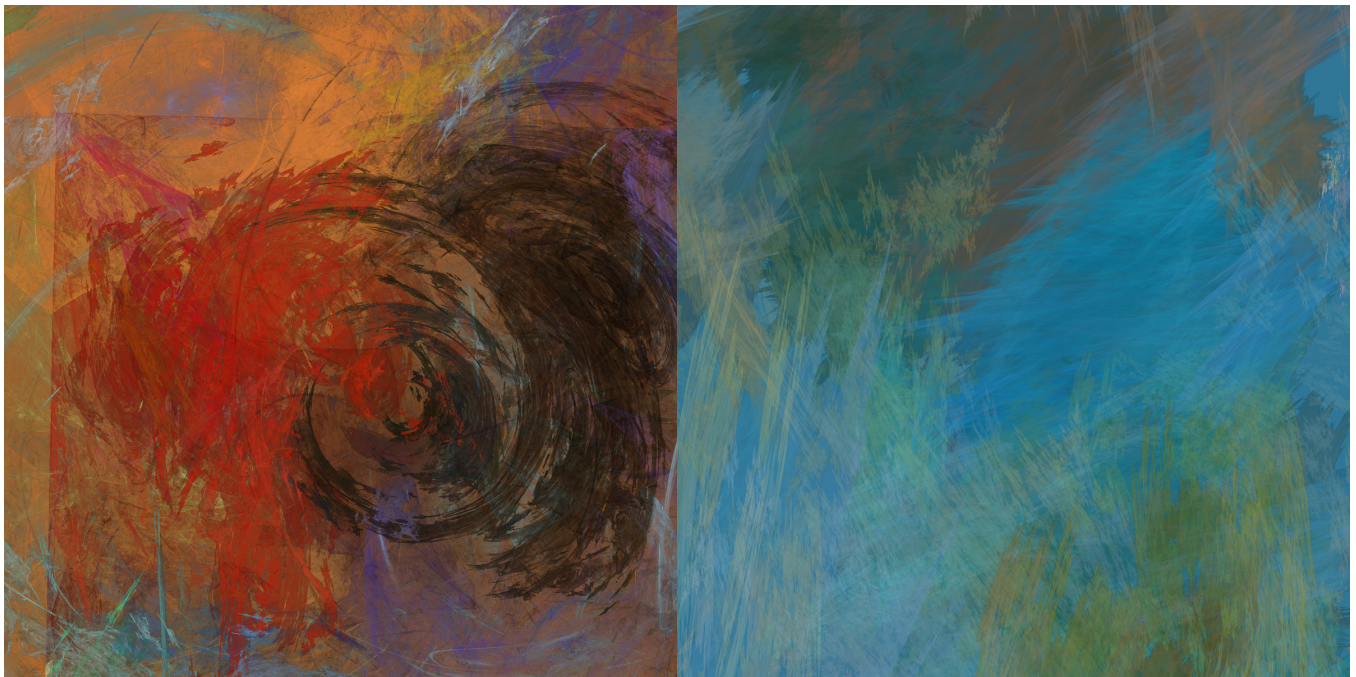


Figure 5: Two fractal flames that were trained on the same reference images as Figure 1 but with modified hyper-parameters. The left fractal was trained at a resolution of 50x50 instead of 200x200. The right fractal was trained with 8 generator functions per flame instead of 24 generator functions.

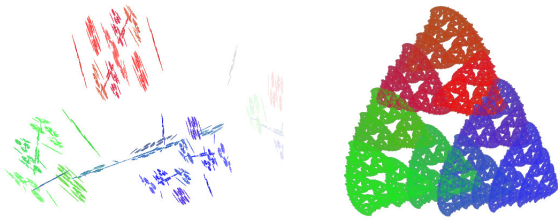


Figure 6: Two linear fractal flames that were trained on the same reference image as Figure 4 but with different hyper-parameters. The left fractal was trained at a resolution of 20x20 instead of 100x100. The right fractal was trained with 3 generator functions instead of 8.

REFERENCES

- Michael Barnsley. 2012. *Fractals Everywhere*. Dover Publications.
- F. Cole, K. Genova, A. Sud, D. Vlastic, and Z. Zhang. 2021. Differentiable Surface Rendering via Non-Differentiable Sampling. In *2021 IEEE/CVF International Conference on Computer Vision (ICCV)*. IEEE Computer Society, Los Alamitos, CA, USA, 6068–6077. <https://doi.org/10.1109/ICCV48922.2021.00603>
- Scott Draves. 1999. Electric Sheep. <https://electricssheep.org>
- Scott Draves and Isabel Walcott Draves. 2010. The flame algorithm and its open source culture. *SIGGRAPH Comput. Graph.* 44, 3 (2010). <https://doi.org/10.1145/1852645.1852650>
- Scott Draves and Erik Reckase. 2008. The fractal flame algorithm. (2008). https://flam3.com/flame_draves.pdf
- Glare Technologies. 2015. Chaotica. <https://www.chaoticafractals.com/>
- Yuanming Hu, Tzu-Mao Li, Luke Anderson, Jonathan Ragan-Kelley, and Frédo Durand. 2019. Taichi: a language for high-performance computation on spatially sparse data structures. *ACM Transactions on Graphics (TOG)* 38, 6 (2019), 201.
- John E. Hutchinson. 1981. Fractals and Self Similarity. *Indiana University Mathematics Journal* 30, 5 (1981), 713–747.
- Diederik P. Kingma and Max Welling. 2014. Auto-Encoding Variational Bayes. In *2nd International Conference on Learning Representations, ICLR 2014, Banff, AB, Canada, April 14-16, 2014, Conference Track Proceedings*.
- Benoit B. Mandelbrot. 1975. *Les objets fractals: forme, hasard et dimension*. Flammarion.
- Franz Marc. 1914. *Fighting Forms*. https://en.wikipedia.org/wiki/File:Fighting_Forms.jpg Public domain.
- Andreas Maschke. 2001. JWildfire. <https://jwildfire.overwhale.com/>
- Claude Monet. 1925. *Wisteria*. https://commons.wikimedia.org/wiki/File:Claude_Monet_-_Wisteria_-_Google_Art_Project.jpg Public domain..
- Rui Qian, Divyansh Garg, Yan Wang, Yurong You, Serge Belongie, Bharath Hariharan, Mark Campbell, Kilian Q. Weinberger, and Wei-Lun Chao. 2020. End-to-End Pseudo-LiDAR for Image-Based 3D Object Detection. In *2020 IEEE/CVF Conference on Computer Vision and Pattern Recognition (CVPR)*. 5880–5889. <https://doi.org/10.1109/CVPR42600.2020.00592>
- Peter Sdobnov, Piotr Borys, and Ronald Hordijk. 2009. Apophysis. <https://sourceforge.net/projects/apophysis/>
- Cheng-Hao Tu, Hong-You Chen, David Carlyn, and Wei-Lun Chao. 2023. Learning fractals by gradient descent. In *Proceedings of the Thirty-Seventh AAAI Conference on Artificial Intelligence (AAAI'23)*. AAAI Press, Article 273. <https://doi.org/10.1609/aaai.v37i2.25342>

Received XXX; revised XXX; accepted XXX

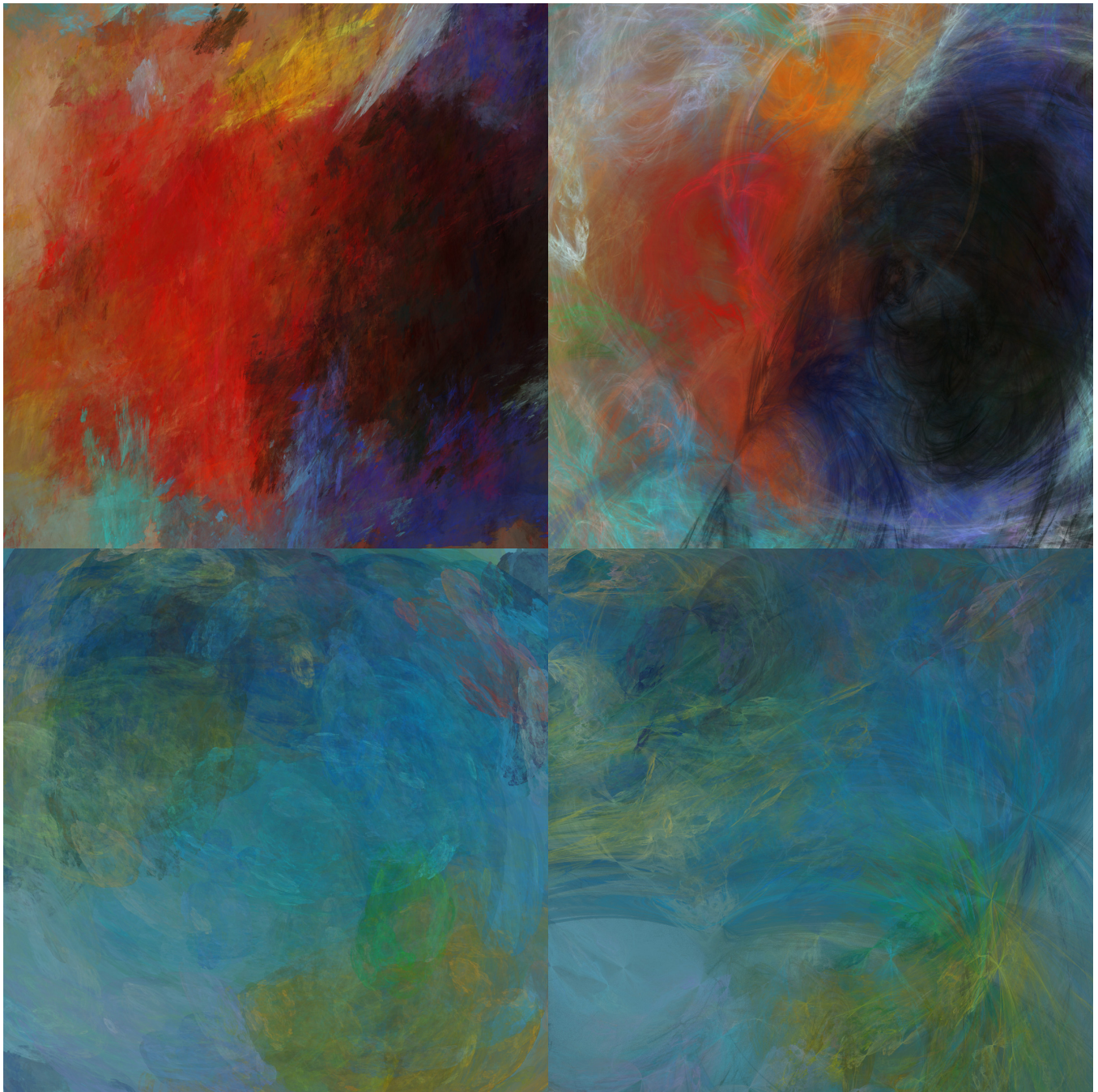


Figure 7: Fractal flames that were trained on the same reference images as Figure 1 but with different generator function variations. Top left: linear variation. Top right: spherical variation. Bottom left: fisheye variation. Bottom right: power variation.